Journal of Southeast University (English Edition) Vol. 31, No. 2, pp. 238 - 243 June 2015 ISSN 1003—7985

Model of limestone calcination/sulfation under oxy-fuel fluidized bed combustion

Wang Chunbo Liu Hongcai Chen Liang

(School of Energy Power and Mechanical Engineering, North China Electric Power University, Baoding 071003, China)

Abstract: The characteristics of the simultaneous calcination/sulfation of limestone under oxy-fuel fluidized bed combustion were studied and compared with those of the sulfation of precalcined CaO. During the calcination stage, SO_2 can react with product CaO and slow down the $CaCO_3$ decomposition rate by the covering effect of the $CaSO_4$ product. The sulfation rate of simultaneous calcination/sulfation is slower than that of precalcined CaO, but with a long enough sulfation time, the calcium conversion of simultaneous calcination/sulfation is higher than that of the precalcined CaO. A grain-micrograin model is established to describe the simultaneous calcination, sintering and sulfation of limestone. The grain-micrograin model can reflect the true reaction process of the calcination and sulfation of limestone in oxy-fuel fluidized bed combustion.

Key words: oxy-fuel; limestone; simultaneous calcination/sulfation; grain-micrograin model

doi: 10.3969/j.issn.1003-7985.2015.02.014

Under the oxy-fuel fluidized bed combustion conditions, CO_2 concentration in flue gas can be enriched up to 80% (air-dry basis) or even higher because of recycle gases. Limestone is usually used for controlling SO_x emission. Furthermore, it can greatly decrease NO_x emissions because there is no N_2 in the combustion atmosphere. Therefore, oxy-fuel combustion is one of promising new technologies that can integrally control the discharge of pollutants by coal combustion[1-3]. The relationship of limestone decomposition temperature and CO_2 partial pressure is[4]

$$\lg p_{co_2} = 7.079 - \frac{8\,308}{T} \tag{1}$$

Under the condition of 80% CO_2, the temperature of the limestone calcined to CaO is 885 ℃, and at the operating temperature (850 ℃) of the conventional CFBB, the sulfation of sorbent is called direct sulfation:

$$CaCO_3 + SO_2 + \frac{1}{2}O_2 \rightarrow CaSO_4 + CO_2 \tag{2}$$

However, when the fuel is petroleum coke or anthracite, the temperature of operation in the furnace is over 900 ℃ and the sulfation occurring in this way is called indirect sulfation:

$$CaCO_3 \rightarrow CaO + CO_2 \tag{3}$$

$$CaO + SO_2 + \frac{1}{2}O_2 \rightarrow CaSO_4 \tag{4}$$

The common experimental method in previous studies concerning reactions (2) and (4) is: First, limestone is calcined to form CaO, and then the sulfation characteristics of CaO are investigated[5-8]. However, under the oxy-fuel CFBB combustion conditions, the CO_2 concentration in flue gas is high, which will delay the decomposition of limestone, and the limestone will be calcined and sulphated simultaneously.

In the past decades, many models were established to simulate the process of calcination and sulfation of limestone. The random pore model was established and used for the reaction of CaO and SO_2 by Bhatia et al.[9-11] and the grain model was founded by Szekely et al[12]. Hartman et al.[13] modified the pore structure. However, most of the sulfation models treat the calcination and sulfation of limestone separately, which is suitable for the sulfation of limestone under the furnace injection conditions due to the high reaction temperature and small particle size causing an instant calcination[14-16]. Yet, they are not appropriate for sulfation in the CFBB when the calcination and sulfation occur simultaneously over a relatively long duration. A combined calcination and sulfation model for reaction of SO_2 and $CaCO_3$ was built[17] to study the calcination and sulfation of limestone integrally under furnace injection conditions, but the applicability of this model to the oxy-fuel CFBB is not clear.

In this work, a grain-micrograin model was used to simulate the process of simultaneous calcination, sintering and sulfation of limestone under the oxy-fuel CFBB conditions. The calcination and sulfation experiments were carried out in a constant temperature tube furnace which can record sample weight change continuously to study the simultaneous calcination and sulfation reactions and verify the model.

Received 2015-01-07.

Biography: Wang Chunbo (1973—), male, doctor, professor, hdwchb@126.com.

Foundation items: The National Natural Science Foundation of China (No. 51276064), the Natural Science Foundation of Hebei Province (No. E2013502292).

Citation: Wang Chunbo, Liu Hongcai, Chen Liang. Model of limestone calcination/sulfation under oxy-fuel fluidized bed combustion[J]. Journal of Southeast University (English Edition), 2015, 31(2): 238 - 243. [doi: 10.3969/j.issn.1003-7985.2015.02.014]

1 Model for Simultaneous Calcination and Sulfation

The grain-micrograin model for the simultaneous calcination and sulfation of limestone is presented and the physical schematic is shown in Fig. 1. The original limestone particles are assumed to be nonporous as shown in Fig. 1(a). $CaCO_3$ grains are calcined from outside to inside and CaO micrograins generate around the uncalcined $CaCO_3$ grain. Meanwhile, CaO micrograins are sintered and sulfated. The SO_2 from bulk gas and CO_2 generated in the decomposition reaction diffuse inside and outside respectively through the pores among CaO micrograins. The $CaSO_4$ product layers was generated around the CaO micrograins, as shown in Fig. 1(b). The heat transfer resistance was ignored in the particle, so the temperature of the particle is equal to the ambient temperature, and gas diffusion resistance from the surface of the particle to bulk gas is also ignored. Pseudo-steady-state approximation is adopted here. According to the analysis above, the grain-micrograin model is described as follows.

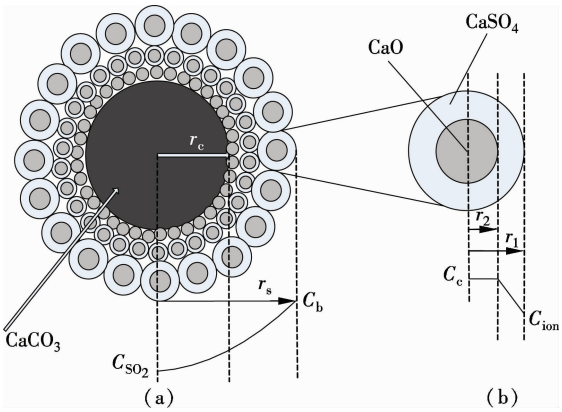

Fig. 1 Grain-micrograin model. (a) The structure of a lomestone grain; (b) A sulfated CaO micrograin

The calcination reaction rate is assumed to be proportional to the reaction rate constant and reaction surface area, and inversely proportional to the CO_2 pressure of the reaction area. So the calcination rate of limestone is

$$V_c = 4\pi r_c^2 \frac{k_c(p_e - p_c)}{p_e} \tag{5}$$

where k_c is the reaction rate constant and p_e is the CO_2 equilibrium partial pressure of limestone. CO_2 generated in the decomposition reaction diffuses outside through the gaps between the CaO micrograins, which can be described by

$$\frac{\partial^2 p}{\partial r^2} + \left(\frac{2}{r} + \frac{1}{D_e}\frac{\partial D_e}{\partial r}\right)\frac{\partial p}{\partial r} + V_C = \frac{\varepsilon_i}{D_e}\frac{\partial p}{\partial t} \tag{6}$$

with the initial conditions $t = 0,\ p = 0$; and the boundary conditions

$$r = r_s,\ p_c = p_b$$

$$r = r_c,\ -D_e\frac{\partial p}{\partial r} = k_c\frac{p_e - p_c}{p_e}$$

where D_e is the effective diffusion coefficient of CO_2 and it is primarily controlled by the Kundsen diffusion,

$$D_e = D_{kc}\varepsilon_i^2 \tag{7}$$

and D_{kc} is the Kundsen diffusion coefficient

$$D_{kc} = 97 r_k\sqrt{\frac{T}{M_{CO_2}}} \tag{8}$$

SO_2 from flue gas diffuses inside through the gaps between the CaO micrograins, which can be described as

$$\frac{1}{r^2}\frac{\partial}{\partial r}\left(r^2 D_{se}\frac{\partial C_{SO_2}}{\partial r}\right) - r_{SO_2} = \frac{\partial C}{\partial t} = 0 \tag{9}$$

with boundary conditions

$$r = r_s,\ C_{SO_2} = C_b$$

$$r = r_c,\ \frac{\partial C_{SO_2}}{\partial R} = 0$$

r_{SO_2} is the sulfation reaction rate, and D_{se} is the effective diffusion coefficient of SO_2 in the CaO particles,

$$D_{se} = D_{ks}\varepsilon_i^2 \tag{10}$$

in which D_{ks} is the Kundsen diffusion coefficient,

$$D_{ks} = 97 r_k\sqrt{\frac{T}{M_{SO_2}}} \tag{11}$$

and r_k is the average pore radius between the CaO micrograins

$$r_k = \frac{2\varepsilon_i}{S_i\rho_{CaO}(1 - \varepsilon_i)} \tag{12}$$

where ε_i is the local porosity of the particle and S_i is the local specific surface area. Due to the sintering and sulfation, the specific surface area and porosity of porous CaO decrease quickly. The sintering rate of CaO is heavily influenced by the specific surface area, which has been investigated by many researchers, and the sintering rate meets the two order dynamic rules[18–19]. So, the change of specific surface area caused by sintering can be calculated by

$$\frac{\mathrm{d}S}{\mathrm{d}t} = -K_{sh}(S - S_a)^2 \tag{13}$$

where S_a is the asymptotic specific surface area with the value of about 5 m^2/g[19], and K_{sh} is the sintering rate constant.

Integrating Eq. (13), we can obtain

$$S = \frac{1}{K_{sh}t + 1/(S_0 - S_a)} + S_a \tag{14}$$

The porosity is related to the specific surface area as

$$\varepsilon = \varepsilon_0\left(\frac{S - S_a}{S_0 - S_a}\right) \tag{15}$$

The local porosity ε_S decreases along with the sulfation reaction because the molar volume of $CaSO_4$ is larger than that of CaO. According to Hartman et al[13], the porosity change can be described as

$$\varepsilon_S = \varepsilon_0 - (Z-1)(1-\varepsilon_0)\chi_S \tag{16}$$

So the local porosity of CaO can be described as

$$\varepsilon_i = \varepsilon_0\left(\frac{S-S_a}{S_0-S_a}\right) - (Z-1)(1-\varepsilon_0)\chi_S \tag{17}$$

with $\varepsilon_0 = 0.54$ and $S_0 = 104\ m^2/g$ according to the investigation of Borgwardt[20]. Z is the molar volume ratio of $CaSO_4$ to CaO, and χ_S is the local sulfation conversion of CaO.

The local specific surface area of CaO particles can be calculated by

$$S_i = \frac{\varepsilon_i}{\varepsilon_0}(S_0 - S_a) + S_a \tag{18}$$

The calcination conversion of $CaCO_3$ to CaO is calculated by

$$X_C = 1 - \left(\frac{r_C}{r_p}\right)^3 \tag{19}$$

in which r_p is the initial radius of $CaCO_3$ grain.

The sulfation rate of CaO can be calculated by

$$r_{CaO} = -\frac{3r_2^2\rho_{CaO}(1-\varepsilon_i)}{r_1^3}\frac{dr_2}{dt} \tag{20}$$

with the initial conditions $t = 0$, $r_1 = r_2 = r_0$.

The sulfation rate of per unit grain volume based on the state ion diffusion obtained by Mahuli[17] is

$$r_{SO_2} = \frac{3k_s}{r_1}(1-\varepsilon_i)C_{ion}C_{SO_2} \tag{21}$$

The sulfation rate of sintered CaO equals the diffusion rate of state ion through the $CaSO_4$ layer according to Lindner[21], so

$$r_{SO_2} = \frac{D_{ion}(C_C - C_{ion})S_{av}}{L} \tag{22}$$

where $L = r_1 - r_2$; D_{ion} is the state ion diffusion coefficient; C_C is the state ion density on the reaction surface equal to the molar density of CaO; and S_{av} is the average cross-sectional area of state ion diffusion.

Combining Eqs. (21) and (22), we obtain the sulfation rate controlled by intrinsic kinetics and product layer state ion diffusion as

$$r_{SO_2} = \frac{3D_{ion}C_C S_{av}k_S(1-\varepsilon_S)C_{SO_2}}{r_1 D_{ion}S_{av} + 3k_S C_{SO_2}(1-\varepsilon_S)(r_1-r_2)} \tag{23}$$

For CaO grains at the same area,

$$r_{SO_2} = r_{CaO} \tag{24}$$

Combining Eqs. (20), (23) and (24), we obtain

$$\frac{dr_2}{dt} = -\frac{D_{ion}S_{av}k_S C_{SO_2}r_1^3}{3r_2^2k_S(1-\varepsilon_S)C_{SO_2}(r_1-r_2) + r_1r_2^2D_{ion}S_{av}} \tag{25}$$

The local sulfation conversion conversion χ_S is

$$\chi_S = 1 - \left(\frac{r_2}{r_0}\right)^3 \tag{26}$$

and the grain size changes along with the sulfation reaction

$$r_1^3 = r_2^3 + Z\chi_S r_0^3 \tag{27}$$

The Ca conversion to $CaSO_4$ can be obtained by integrating local conversion conversion of all layers, so

$$X_S = \frac{3\int_{r_c}^{r_s}\chi_S r^2\,dr}{r_S^3} \tag{28}$$

The relative quality change at the simultaneous calcination and sulfation is

$$\frac{w}{w_0} = 1 - \frac{M_{CaCO_3} - M_{CaO}}{M_{CaCO_3}}X_C + \frac{M_{CaSO_4} - M_{CaO}}{M_{CaCO_3}}X_S \tag{29}$$

2 Experiment Facility and Procedure

The isothermal thermo-gravimetric experiment system to investigate simultaneous calcination and sulfation of limestone at constant temperature is shown in Fig. 2. The tube furnace is 40 mm in diameter and 800 mm in length. The temperature in the furnace was monitored by an automatic controller with a range of 20 to 1 200 ℃. The change of sample weights was monitored by the computer constantly and the precision of the weight sensor was 0.1 mg. Simulated flue gas consists of 75% CO_2, 5% O_2, 0.2% SO_2 and N_2 as balance. In all tests, the flow rate of the gas mixtures was maintained at 1 200 mL/min. This flow rate is selected as it has been verified that at this flow rate, the mass transfer is not the limiting factor for the reactions. Previous work[22-23] operated on this device has verified that it has sufficient accuracy.

Shandian limestone was used in the experiment. The X-ray fluorescence (XRF) analysis result of limestone is given in Tab. 1. A known amount of limestone sample (about 80 mg) was loaded into a quartz boat (100 mm in length, 10 mm in width and 10 mm in depth). In order to be close to the working conditions of industry as much as possible, the temperature was raised to the desired level and maintained for 60 min, and then the quartz boat (with limestone) was sent into the furnace quickly.

Tab. 1 Main component of limestone %

$w(CaCO_3)$	$w(MgCO_3)$	$w(Fe_2O_3)$	$w(SiO_2)$	$w(Al_2O_3)$
95	2.24	0.47	1.92	0.37

The calcium conversion of sample (after limestone decomposes into CaO completely) is calculated by

$$X = \left(\frac{m_t - m_0}{m_i A}\right)\left(\frac{w_{CaCO_3}}{w_{CaSO_4} - w_{CaO}}\right) \tag{30}$$

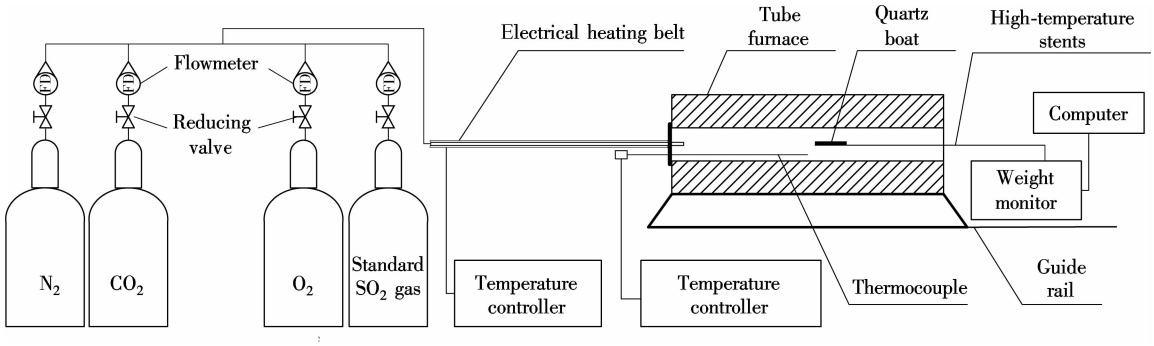

Fig. 2 Experimental system

where X is the conversion of calcium; m_t is the mass at the time t; m_0 is the original sample mass of CaO formed by calcined limestone without SO_2; m_i is the initial sample mass of limestone; A is the mass fraction of the $CaCO_3$ in the original samples; w_{CaCO_3}, w_{CaSO_4} and w_{CaO} are the molar mass of $CaCO_3$, $CaSO_4$ and CaO, respectively.

The experiments of simultaneous calcination and sulfation (termed simultaneous calcination/sulfation) are carried out with 0.2% SO_2; and are compared, experiments in which limestone calcined in pure N_2 to CaO and then sulfated (termed calcination-sulfation) with 0.2% SO_2 are also given.

3 Results and Discussion

The characteristics of simultaneous calcination/sulfation and calcination-sulfation along with the calculation result of the model is shown in Fig. 3.

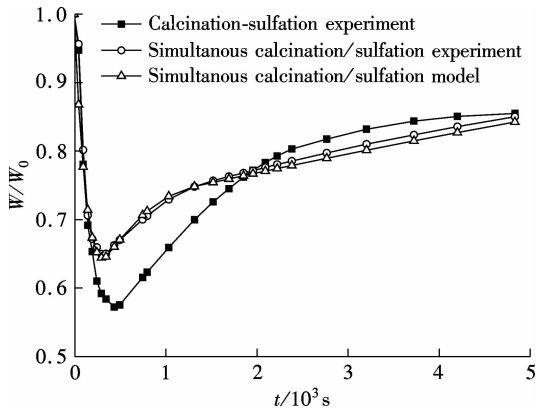

Fig. 3 Tesing and model prediction (900 ℃, 150 to 250 μm, 0.2% SO_2, 5% O_2, 75% CO_2, N_2 as balance)

Fig. 3 shows the ratio of sample weight W to the initial weight W_0 in the process of experiment. First, a significant difference can be found when comparing the experimental data of calcination-sulfuration to those of the simultaneous calcination/sulfation reaction. Compared with calcination-sulfuration, the weight loss rate of simultaneous calcination/sulfation in the weight decline stage is slightly slower, but the lowest weight point is obviously higher. The cause is that the calcination and sulfation reaction occurs at the same time in the calcination stage of the simultaneous calcination/sulfation experiment, which, on the one hand, increases the sample weight due to the sulfation of CaO; and on the other hand, prevents the calcination of $CaCO_3$ by the product layer of $CaSO_4$. What should be pointed out is that when calcination and sulfation occur simultaneously, the limestone loses weight due to calcination but gains weight by sulfation; which can lead to the result that the lowest weight point is not the point that limestone is calcined completely usually, but only a balance point between weight gain and loss.

The next significant difference obtained from Fig. 3 is that during the period of weight rise, although there remains two reaction stages which include a fast reaction stage controlled by reaction kinetics and a slow reaction stage controlled by product layer diffusion for both of the two experimental conditions; the percentage of weight gain is relatively lower in the early stage and higher in the later stage for simultaneous calcination/sulfation experiments.

The calculating results of the grain-micrograin model established is consistant with the testing results and can be used to describe the simultaneous calcination and sulfation of limestone, as shown in Fig. 3. Even if in pure N_2, it needed about 500 s for the limestone particle of 150 to 250 μm to be calcined completely. Therefore, it is necessary to take the sulfation of CaO into account in this long calcination stage, because not only the calcination of $CaCO_3$ but also the sulfation of CaO are influenced by it. Data will not reflect reality if sulfation of the precalcined CaO is taken as the sulfation of limestone in an oxy-fuel CFBC. Simultaneous sulfation with calcination of limestone should not be ignored for both experiment and model derivation when studying sulfation phenomenon in oxy-fuel CFBB.

To calculate the sulfation ratio of limestone, it must be ensured that all $CaCO_3$ in the sample is calcined to CaO completely. To detect if there is $CaCO_3$ in the samples, several samples undergoing different reaction times after the lowest weight point are quickly cooled in N_2 to room temperature and grinded to less than 10 μm, and then cal-

cined again at 900 ℃ in pure N_2 within sufficient time. If a sample does not lose weight in this process, it can be ensure that there is no $CaCO_3$ in the sample. Also, the test results show that the samples after 680 s do not lose mass anymore, which means that there is no $CaCO_3$ in these samples. So, the calcium conversion formula can be used to calculate the calcium conversion to $CaSO_4$, as shown in Fig. 4.

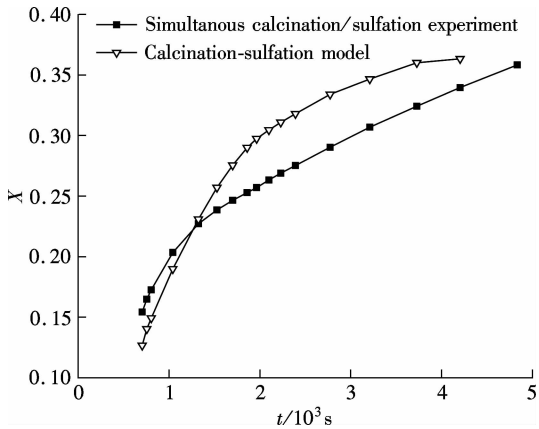

Fig. 4 Conversion for simultaneous calcinations/sulfation and calcinations-sulfation of limestone

From Fig. 4, it can be shown that the sulfation rate of calcination-sulfation experiment was faster at first but declined quickly when compared with simultaneous calcinations/sulfation. Although the calcium conversion of calcination-sulfation is higher after the cross point in Fig. 4, its conversion rate slowed down finally, so if with a longer reaction time, the conversion of simultaneous calcinations/sulfation should exceed that of calcinations-sulfation.

Perhaps one contrast test is not sufficient to illustrate the problems, so several other contrast tests and model calculations are carried out, and Fig. 5 and Fig 6 show two of them.

Fig. 5 is the result of experiment and model calculation for a particle size of 75 to 97 μm, and Fig. 6 is for a temperature of 950 ℃ compared with Fig. 4. It can be found

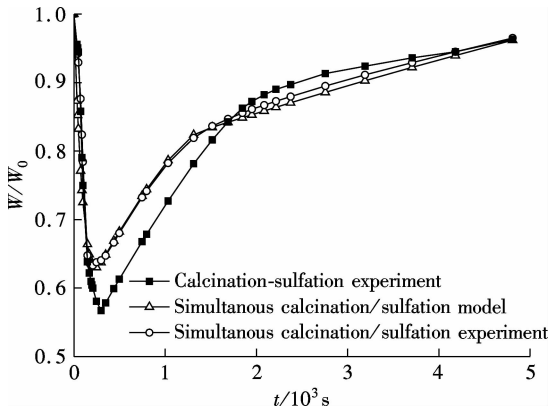

Fig. 5 Tesing and model prediction (900 ℃, 75 to 97 μm, 0.2% SO_2, 5% O_2, 75% CO_2, N_2 as balance)

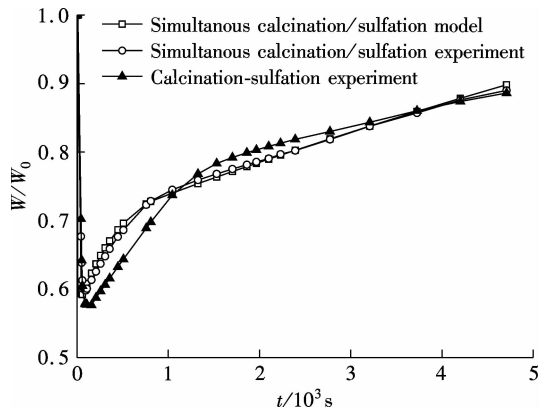

Fig. 6 Tesing and model prediction (950 ℃, 150 to 250 μm, 0.2% SO_2, 5% O_2, 75% CO_2, N_2 as balance)

that a similar phenomenon occurs for different experimental temperatures and particle sizes, which illustrates that the differences between simultaneous calcination/sulfation and calcination-sulfation conditions are not an accidental phenomenon. The grain-micrograin model established in this work can also describe the true process of simultaneous calcination/sulfation under different experimental conditions.

4 Conclusion

The simultaneous calcination/sulfation of limestone under oxy-fuel fluidized bed combustion conditions is different from the sulfation of CaO. Also, during the calcination stage, SO_2 will slow down the $CaCO_3$ decomposition rate via the covering effect of the $CaSO_4$ product. The sulfation rate of simultaneous calcination/sulfation declines slower than that of precalcined CaO, and with a long enough sulfation time, the calcium conversion of simultaneous calcination/sulfation is higher than that of precalcined CaO. The grain-micrograin model combining simultaneous calcination, sintering and sulfation can reflect the true process of the calcination and sulfation of limestone under an oxy-fuel fluidized bed combustion. When studying the calcination and sulfation of limestone under oxy-fuel CFBB conditions, it is necessary to pay attention to the calcination and sulfation of limestone at the same time.

References

[1] Liu H, Okazaki K. Simultaneous easy CO_2 recovery and drastic reduction and NO_x in O_2/CO_2 coal combustion with heat recirculation[J]. *Fuel*, 2003, **82**(11): 1427 – 1436.

[2] Liu Hao, Ren Ruiqi, Huang Yongjun, et al. Reduction and emission of NO in oxy-fuel system[J]. *Journal of Chemical Industry and Engineering*, 2011, **62**(2): 495 – 501. (in Chinese)

[3] Duan Lunbo, Zhou Wu, Qu Chengrui, et al. SO_2 emission from a coal-fired circulating fluidized bed combustor under O_2/CO_2 atmosphere[J]. *Journal of Engineering*

Thermophysics, 2012, **33**(1): 151 - 154.
[4] Baker E H. The calcium oxide-carbon dioxide system in the pressure range 1-300 atmopheres[J/OL]. *Journal of the Chemical Society (Resumed)*, 1962: 464 - 470. http://pubs. rsc. org/en/content/articlepdf/1962/jr/jr9620000464.
[5] Wang W Y, Bjerle I. Modeling of high-temperature desulfurization by Ca-based sorbents[J]. *Chemical Engineering Science*, 1998, **53**(11): 1973 - 1989.
[6] Wang C, Jia L, Tan Y, et al. The effect of water on the sulfation of limestone[J]. *Fuel*, 2010, **89**(9): 2628 - 2632.
[7] Stewart M C, Manovic V, Anthony E J, et al. Enhancement of indirect sulfation of limestone by steam addition [J]. *Environmental Science and Technology*, 2010, **44** (22): 8781 - 8786.
[8] García-Labiano F, Rufas A, de Diego L F, et al. Calcium-based sorbents behaviour during sulfation at oxy-fuel fluidised bed combustion conditions[J]. *Fuel*, 2011, **90** (10): 3100 - 3108.
[9] Bhatia S K, Perlmutter D D. A random pore model for fluid-solid reactions: Ⅰ. Isothermal, kinetic control[J]. *AIChE Journal*, 1980, **26**(3): 379 - 386.
[10] Bhatia S K, Perlmutter D D. A random pore model for fluid-solid reactions: Ⅱ. Diffusion and transport effects [J]. *AIChE Journal*, 1981, **27**(2): 247 - 254.
[11] Bhatia S K, Perlmutter D D. The effect of pore structure on fluid-solid reactions: application to the SO_2-lime reaction[J]. *AIChE Journal* 1981, **27**(2): 226 - 234.
[12] Szekely J, Evans J W. A structural model for gas-solid reactions with a moving boundary[J]. *Chemical Engineering Science*, 1970, **25**(6): 1091 - 1107.
[13] Hartman M, Coughlin R W. Reaction of sulfur dioxide with limestone and the grain model[J]. *AIChE Journal*, 1976, **22**(3): 490 - 498.
[14] Silcox G D, Kramlich J C. A mathematical model for the flash calcination of dispersed $CaCO_3$ and $Ca(OH)_2$ particles [J]. *Industrial Engineering Chemistry Research*, 1989, **28**(2): 155 - 160.
[15] Milne C R, Silcox G D, Pershing D W, et al. High-temperature, short-time sulfation of calcium-based sorbents. 1. Theoretical sulfation model[J]. *Industrial Engineering Chemistry Research*, 1990, **29**(11): 2192 - 2201.
[16] Milne C R, Silcox G D, Pershing D W, et al. High-temperature, short-time sulfation of calcium-based sorbents. 2. Experimental data and theoretical model predictions [J]. *Industrial Engineering Chemistry Research*, 1990, **29** (11): 2201 - 2214.
[17] Mahuli S K, Agnihotri R, Jadhav R, et al. Combined calcination, sintering and Sulfation model for $CaCO_3$ SO_2 reaction[J]. *AIChE Journal*, 1999, **45**(2): 367 - 382.
[18] Ghosh-Dastidar A, Mahuli S, Agnihotri R, et al. Ultrafast calcination and sintering of $Ca(OH)_2$ powder: experimental and modeling[J]. *Chemical Engineering Science*, 1995, **50**(13): 2029 - 2040.
[19] Agnew J, Hampartsoumian E, Jones J M, et al. The simultaneous calcination and sintering of calcium based sorbents under a combustion atmosphere[J]. *Fuel*, 2000, **79** (12): 1515 - 1523.
[20] Borgwardt R H. Sintering of nascent calcium oxide[J]. *Chemical Engineering Science*, 1989, **44**(1): 53 - 60.
[21] Lindner B, Simonsson D. Comparison of structural models for gas-solid reactions in porous solids undergoing structural changes [J]. *Chemical Engineering Science*, 1981, **36**(9): 1519 - 1527.
[22] Wang Chunbo, Zhang Yue, Jia Lufei, et al. Effect of water vapor on the pore structure and sulfation of CaO [J]. *Fuel*, 2014, **130**: 60 - 65.
[23] Wang Chunbo, Wang Jinxing, Lei Ming, et al. Investigations on combustion and NO emission characteristics of coal and biomass blends[J]. *Energy & Fuel*, 2013, **27** (10): 6185 - 6190.

富氧燃烧循环流化床中石灰石煅烧/硫化反应模型

王春波　刘洪才　陈　亮

(华北电力大学能源动力与机械工程学院,保定 071003)

摘要:对富氧燃烧流化床下石灰石同时煅烧/硫化特性进行了研究,并与 CaO 硫化特性进行了比较. 在石灰石煅烧阶段,CaO 与 SO_2 反应生成 $CaSO_4$ 产物层覆盖在未煅烧 $CaCO_3$ 的外层,降低了煅烧速率. 同时煅烧/硫化过程中的硫化反应速率比 CaO 的硫化反应速率要缓慢,但是经过足够长的反应时间后,同时煅烧/硫化反应的钙转化率比 CaO 硫化反应的钙转化率要高. 建立了一个包含石灰石同时煅烧、烧结和硫化反应的晶粒-微晶粒模型用于描述流化床内同时进行的石灰石煅烧、烧结和硫化过程,实验证明所建立的模型能够反映流化床富氧气氛中石灰石的真实煅烧/硫化过程.

关键词:富氧燃烧;石灰石;同时煅烧/硫化;晶粒-微晶粒模型

中图分类号:TK16